Zero Time Delay Input Shaping for Smooth Settling of Industrial Robots*

Yu Zhao[1], Wenjie Chen[2], Te Tang[1], and Masayoshi Tomizuka[1]

Abstract— **Precise motion control is desired in a variety of industrial robot applications. In order to achieve precise and rapid rest-to-rest motion, the overshoot and the residual vibration should be minimized. In this paper, a modified input shaping approach is developed to address these problems. The time delay introduced by conventional input shaping technique is fully compensated in the proposed approach. Experiment result on an industrial robot has shown the effectiveness of the proposed approach.**

I. INTRODUCTION

Industrial robots are widely used in manufacturing. In order to guarantee high product quality, as well as high productivity, precision position control and rapid rest-to-rest motion are desired in a variety of applications. However, serious overshoots and residual vibrations are widely and frequently observed when industrial robots are conducting fast motions [1]. Flexibility introduced by transmission units is the major cause of these unwanted motions [2]. In order to improve trajectory tracking performance, the overshoot and the residual vibration must be minimized, and the flexibility of industrial robots must be taken into account in the controller design .

To address these problems, several approaches are proposed, including singular perturbation [3], optimal trajectory planning [4], input shaping [5]–[7], nonlinear feedback control [8], [9], and iterative learning control [10], [11]. With a sophisticated system model, optimal trajectory planning can be implemented to generate an optimal motion reference to minimize the overshoot and the residual vibration. If such kind of model is not available, but the states related to the elastic vibration can be measured or observed, singular perturbation and nonlinear feedback control may be implemented to accommodate unmodeled dynamics and disturbances. Iterative learning control is another choice to address these problems by learning an optimal feedforward control when robot performs the same task repeatedly.

Comparing to other approaches, input shaping, which is also known as command shaping, may be implemented to effectively minimize the overshoot and the residual vibration a) without a sophisticated dynamical model; b) without directly measuring elastic vibrations for online feedback; c) without requirement of repeated tasks. Input shaping was first proposed for smoothing or shaping the inputs of linear second order systems. Later, modifications and extensions were introduced to handle multiple modes and changing natural frequencies of the system [12]. The robustness of input shaping was also considered to accommodate parameter uncertainty and disturbances [13].

As one of the easiest and successfully applied feedforward control techniques, input shaping has been implemented in a variety of applications ranging from nano-positioning devices to large industrial cranes [14]–[16]. However, there are certain drawbacks of input shaping for industrial robot applications. One drawback is the time delay introduced by input shaping. For industrial robots performing rapid rest-to-rest motions, the time delay could slow down the entire task, which is not desired in industrial applications. Another drawback is that input shaping may change the original motion reference. In certain applications, like spot welding, an industrial robot is required to move along a pre-specified trajectory to avoid colliding with work-pieces. If the shaped motion command does not is also considered in the design of the proposed input shaping approach. Experiment results on a 6-axis industrial robot has verified the effectiveness of the proposed approach. preserve the path of the original trajectory, there could be collision between the robot and the work-pieces. In order to compensate the time delay, this paper proposes a zero time delay

This paper is organized as follows: conventional input shaping techniques are reviewed in Section II; the proposed zero time delay input shaping approach is introduced in Section III; experiment results on a 6-axis industrial robot is shown in Section IV; Section V concludes this paper.

II. INPUT SHAPING

A review of conventional input shaping techniques is provided in this section [6], [7], [13]. Input shaping is implemented by convolving a sequence of impulses with the original system input. Each impulse can excite an oscillatory response. When the amplitudes and time delays are well tuned such that the oscillatory responses cancel each other, there will be no residual vibration.

The idea of input shaping was first introduced for linear second order systems. Consider a linear second order system with the transfer function G,

$$G(s) = \frac{K\omega_0^2}{s^2 + 2D\omega_0 s + \omega_0^2} \tag{1}$$

where ω_0 is the natural frequency, D is the damping ratio, and K is the static gain. The unit impulse response $y(t)$ of

*This work was supported by FANUC Corporation

[1]Yu Zhao, Te Tang, and Masayoshi Tomizuka are with the Department of Mechanical Engineering, University of California at Berkeley, Berkely, CA 94720, USA. E-mail: {yzhao334, tetang}@berkeley.edu, tomizuka@me.berkeley.edu.

[2]Wenjie Chen is with the FANUC Corporation, Oshino-mura, Yamanashi Prefecture, 401-0597, Japan

this linear second order system (1) is

$$y(t) = K\frac{\omega_0}{\sqrt{1-D^2}}e^{-\omega_0 Dt}\sin(\omega_d t) \tag{2}$$

where $\omega_d = \omega_0\sqrt{1-D^2}$ is the damped natural frequency.

Let f_{IS} be a sequence of n impulses

$$f_{IS}(t) = \sum_{i=1}^{n} A_i\delta(t-t_i) \tag{3}$$

where A_i is the amplitude of the i^{th} impulse, t_i is the time delay of the i^{th} impulse. Typically, it is assumed that

$$\begin{array}{rcl} t_{i+1} & > & t_i \\ A_i & > & 0 \end{array} \tag{4}$$

Convolving this sequence with the original unit impulse, the resulting response $Y_{IS}(t)$ for $t \geq t_n$ is

$$\begin{array}{rcl} Y_{IS}(t) & = & \sum_{i=1}^{n} A_i y(t-t_i) \\ & = & K\frac{\omega_0}{\sqrt{1-D^2}}e^{-\omega_0 Dt}[A(\omega_0,D)\sin(\omega_d t) \\ & & \qquad -B(\omega_0,D)\cos(\omega_d t)] \\ & = & K\frac{\omega_0}{\sqrt{1-D^2}}e^{-\omega_0 Dt}I(\omega_0,D)\sin(\omega_d t+\phi) \end{array} \tag{5}$$

where

$$\begin{array}{rcl} I(\omega_0,D) & = & \sqrt{A(\omega_0,D)^2+B(\omega_0,D)^2} \\ A(\omega_0,D) & = & \sum_{i=1}^{n} A_i e^{\omega_0 Dt_i}\cos(\omega_d t_i) \\ B(\omega_0,D) & = & \sum_{i=1}^{n} A_i e^{\omega_0 Dt_i}\sin(\omega_d t_i) \\ \cos(\phi) & = & \frac{A(\omega_0,D)}{I(\omega_0,D)} \\ \sin(\phi) & = & -\frac{B(\omega_0,D)}{I(\omega_0,D)} \end{array} \tag{6}$$

The amplitude ratio between the shaped impulse response (5) and unshaped impulse response (2) after t_n is typically used as the performance index of input shaping [13]. This ratio is also known as percentage of residual vibration, which is defined as

$$\begin{array}{rcl} V(\omega_0,D) & := & e^{-\omega_0 Dt_n}\sqrt{A(\omega_0,D)^2+B(\omega_0,D)^2} \\ & = & e^{-\omega_0 Dt_n}I(\omega_0,D) \end{array} \tag{7}$$

The term $e^{-\omega_0 Dt_n}$ implies that a time delay t_n is introduced in the shaped response. This ratio reflects the effect of the residual vibration suppression. The design objective of input shaping is to make $V \approx 0$.

For a given system, V depends only on the amplitudes and time delays of the sequence of impulses f_{IS}. Therefore the design of input shaping is equivalent to the design of the sequence f_{IS}, which is also known as an input shaper.

One design of the input shaper is called zero vibration (ZV) shaper. There are only two impulses in a ZV shaper. The design of a ZV shaper involves solving a set of equations with constraints (4)

$$\begin{array}{rcl} A(\omega_0,D) & = & 0 \\ B(\omega_0,D) & = & 0 \\ \sum_{i=1}^{n} A_i & = & 1 \end{array} \tag{8}$$

where the first two equations are derived from that the percentage of residual vibration $V = 0$, and the third equation is derived from the requirement that the input shaper has an unity static gain for avoiding overshoot. The design of a ZV shaper can be chosen as the solution of (8) with the minimum t_2.

Theoretically, ZV shaper could completely eliminate the residual vibration since $V = 0$ for accurately known ω_0, D. However, ZV shaper can be sensitive to modeling errors in practice. Thus robust design of input shaping was considered. Zero vibration and derivative (ZVD) shaper, extra-insensitivity (EI) shaper, and specified insensitivity (SI) shaper are commonly used robust input shapers [17]. Only the specified insensitivity shaper is reviewed here since it provides the most robust performance in these approaches.

The design of SI shaper can be stated as an optimization problem. The objective is to minimize the total time delay of the input shaping. On one hand, the constraints of this optimization problem come from (4). On the other hand, the constrains of this optimization problem come from the requirement of SI that the percentage of residual vibration is below a given level within a range of frequencies. It is difficult to derive the analytical form of the percentage of residual vibration constraint. Instead, an approximate approach called frequency sampling approach is typically implemented in the design of SI shaper.

In the frequency sampling approach, it is assumed that the natural frequency satisfies $\omega_0 \in [\omega_{inf}, \omega_{sup}]$, and the resulting percentage of residual vibration is required to be below a given level V_0. A set of frequencies are sampled from the frequency range as $\{\omega_0^1, \omega_0^2, \cdots, \omega_0^m\}$, where m is the number of samples, and ω_0^i is the i^{th} frequency sample. Suppose n impulses are used in the shaper, the design of SI shaper can be formulated as

$$\begin{array}{rl} \min\limits_{A_1,\cdots,A_n,t_1,\cdots,t_n} & t_n \\ s.t. & t_{i+1} > t_i, i = 1,\cdots,n \\ & A_i > 0, i = 1,\cdots,n \\ & \sum_{i=1}^{n} A_i = 1 \\ & V(\omega_0^j, D) \leq V_0, j = 1,\cdots,m \end{array} \tag{9}$$

When the sample set is large enough to cover the frequency range, the frequency range $[\omega_{inf}, \omega_{sup}]$ can be well approximated by the samples. In actual application, as long as the estimated natural frequency is in the frequency range, SI shaper guarantees good residual vibration suppression performance. The cost of such robust input shaper is longer time delay. Usually more than two impulses should be implemented, and the overall time delay is longer than ZV shaper.

III. Zero Time Delay Input Shaping

The proposed zero time delay input shaping is introduced in this section. A path constraint issue of implementing input shaping on industrial robot is firstly addressed. The zero time delay input shaping is then developed based on the path constraint design.

A. Input Shaping with Path Constraint

In many works, input shaping is applied on single-input single-output systems. In this paper, input shaping is implemented on a 6-axis industrial robot, which is a multiple-input multiple-output system. One natural choice is to implement input shaping on each axis independently. However, as mentioned in the introduction, this may change the original task space motion reference, which could result in undesired behaviour of the robot.

For the motion command given in Cartesian space, another intuitive approach is to apply input shaping to the Cartesian space motion command of industrial robots. The corresponding joint space motion command can be obtained through the solution of inverse kinematics problem. However, input shaping is "smoothing" the motion command in each direction of the Cartesian space, thus the shaped motion path can still be different from the original motion path.

In this paper, a third approach is developed. Let the Cartesian space motion command be $\{x(t), y(t), z(t)\}$, where the motion time $t \in [0, T]$. The motion command can be parametrized with the normalized arc length s, defined as

$$s(t) = \frac{\int_{\tau=0}^{t} \sqrt{\dot{x}(\tau)^2 + \dot{y}(\tau)^2 + \dot{z}(\tau)^2}\, d\tau}{\int_{\tau=0}^{T} \sqrt{\dot{x}(\tau)^2 + \dot{y}(\tau)^2 + \dot{z}(\tau)^2}\, d\tau} \tag{10}$$

where $s \in [0, 1]$. The motion command can be parametrized as $\{x(s), y(s), z(s)\}$. Input shaping is then implemented on the normalized arc length $s(t)$. The corresponding joint space motion command is then obtained through the solution of inverse kinematics problem.

A comparison of input shaping on joint space motion command, Cartesian space motion command, proposed approach, and the unshaped motion command is given in Fig.1.

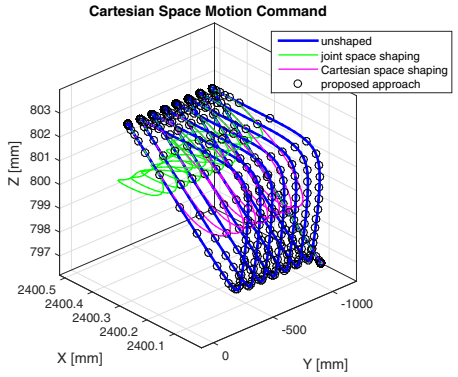

Fig. 1: Comparison of Input Shaping on Joint Space Motion Command, Cartesian Space Motion Command, and the Proposed Approach.

As shown in the figure, directly implementing input shaping to joint space motion command results in a large deviation. Implementing input shaping in Cartesian space makes the shaped motion command closer to the unshaped motion command, but the deviation still exists. The proposed approach preserves the path of the unshaped motion command.

B. Zero Time Delay Shaping

In order to preserve the path of unshaped motion command, the proposed approach in III-A is implemented. The input to the system can be chosen as the normalized arc length $s(t), t \in [0, T]$. Input shaping is then implemented on the normalized arc length. According to the existing literature, time delay will be inevitably introduced by traditional input shaping. If robustness is considered in the design, the time delay could be even longer. In order to eliminate the undesired time delay, and keep the robust design of input shaping at the same time, the following design procedure is proposed:

1. Design an input shaping using any approach introduced in the literature. The input shaper $f_{IS} = \sum_{i=1}^{n} A_i \delta(t - t_i)$ is obtained. The time delay introduced by the input shaping is t_n.
2. Accelerate the unshaped motion command $s(t)$ to $s_{acc}(\tau)$, where $t \in [0, T]$, $\tau \in [0, T - t_{acc}]$, and $t_n < t_{acc} < T$.
3. Apply the input shaping designed in the first step to the accelerated motion command $s(\tau)$. The resulting shaped input is $S_{IS} = f_{IS} * s_{acc}$.

For the second step, let a time scale parameter be $k = \frac{T - t_{acc}}{T} < 1$, the accelerated normalized arc length is

$$s_{acc}(\tau) = s_{acc}(kt) = s(t), t \in [0, T] \tag{11}$$

Suppose there are n impulses in the input shaper (3). The resulting shaped motion command is

$$S_{IS}(t') = \sum_{i=1}^{n} A_i s'_{acc}(t' - t_i) \cdot u(t' - t_i) \tag{12}$$

where the time variable $t' \in [0, T - t_{acc} + t_n]$; $s'_{acc}(t')$ is an extension of s_{acc} such that

$$s'_{acc}(t') = \begin{cases} s_{acc}(t'), & t' \in [0, T - t_{acc}] \\ s_{acc}(T - t_{acc}), & t' \geq T - t_{acc} \end{cases}$$

and $u(t')$ is the Heaviside step function that

$$u(t') = \begin{cases} 0, & t' < 0 \\ 1, & t' \geq 0 \end{cases}$$

Comparing to the unshaped motion command $s(t), t \in [0, T]$, the shaped motion command ends at $T - t_{acc} + t_n$. Since $t_{acc} > t_n$, the end time of the shaped motion command satisfies $T - t_{acc} + t_n < T$.

The proposed input shaping approach is sketched in Fig.2. As shown in the figure, the unshaped motion command is first accelerated. After input shaping is applied, time delay is introduced to the accelerated motion command, but there is no time delay between the unshaped motion command and the shaped motion command.

The velocity or changing rate of the motion commands are compared in Fig.3. As shown in the figure, it is clear that the shaped motion command ends earlier than the unshaped motion command, which means that there is no time delay when applying this approach.

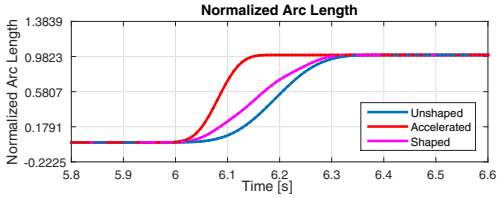

Fig. 2: Shape of Arc Length.

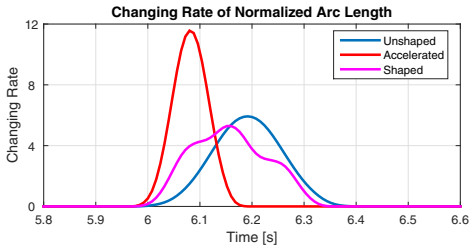

Fig. 3: Shape of Arc Velocity.

IV. Implementation and Experiment Result

The proposed approach is implemented on a 6-axis industrial robot as shown in Fig.4.

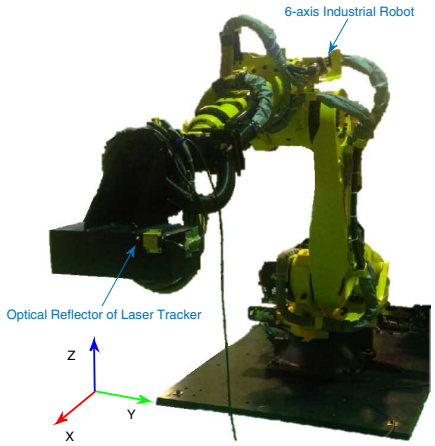

Fig. 4: 6-Axis Industrial Robot.

The robot is performing a rapid rest-to-rest motion (e.g., a typical spot welding motion). The optical reflector of an laser tracker is attached to the tool center point of the robot for measuring the endeffector motion. The Cartesian space motion command and the position measurement from the laser tracker is shown in Fig.5. There exists obvious overshoot and residual vibration.

A. Frequency and Damping Ratio Estimation

The natural frequency and damping ratio are required for the design of input shaping. The motion data measured by the laser tracker is used to estimate these parameters. The residual vibration of the robot is considered to be caused by the flexibility at each joint of the robot. It is assumed that

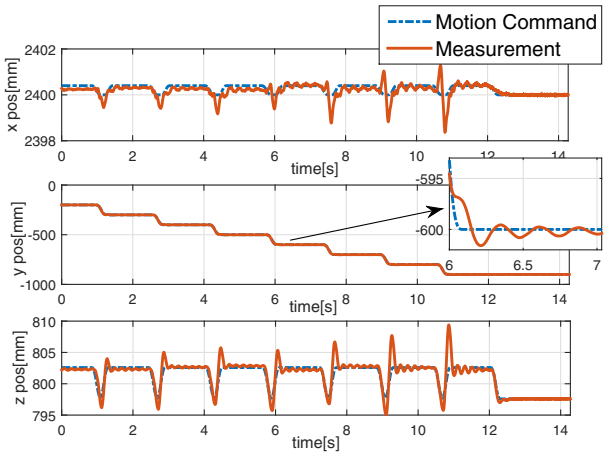

Fig. 5: Cartesian Space Motion Command and the Position Measurement.

the residual vibration of each joint can be fitted into a free vibration of a mass-spring-damper system, which is a linear second order system. No angular velocity in Cartesian space is measured in the experiment, thus the joint space velocity is assumed to be calculated using

$$\dot{q} = J(q)^{-1} \begin{bmatrix} \dot{p} \\ 0 \end{bmatrix} \tag{13}$$

where $q = [q_1, \cdots, q_6]^T$ is the set of joint positions of the robot; $J(q)$ is the Jacobian matrix of the robot; $p = [x, y, z]^T$ is measured Cartesian space position of the robot, in which x, y, z are the Cartesian space position in x, y, z direction. The calculated joint space velocities during the one of the residual vibrations in the entire motion are shown in Fig.6.

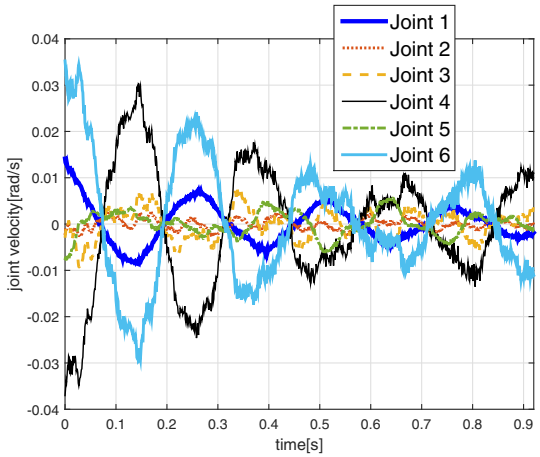

Fig. 6: Estimated Joint Velocity During One of the Residual Vibrations.

Let the time domain response of the free vibration of the linear second order system (1) be $\eta(t)$.

$$\eta(t) = e^{-D\omega_0 t} \left(C_1 \cos(\omega_d t) + C_2 \sin(\omega_d t)\right) \tag{14}$$

where

$$\begin{aligned} C_1 &= \eta(0) \\ C_2 &= \frac{\dot{\eta}(0)+D\omega_0\eta(0)}{\omega_d} \end{aligned} \tag{15}$$

The velocity of the free vibration of a linear second order system (1) is

$$\begin{aligned} \dot{\eta}(t) &= -D\omega_0 e^{-D\omega_0 t}\left(C_1\cos(\omega_d t)+C_2\sin(\omega_d t)\right) \\ &\quad \omega_d e^{-D\omega_0 t}\left(C_2\cos(\omega_d t)-C_1\sin(\omega_d t)\right) \end{aligned} \tag{16}$$

The frequency and damping parameters of each joint is first roughly estimated using fast Fourier transformation (FFT). These parameters are further tuned to fit (16) using least squares method. The fitting result is illustrated by one of the results as shown in Fig.7.

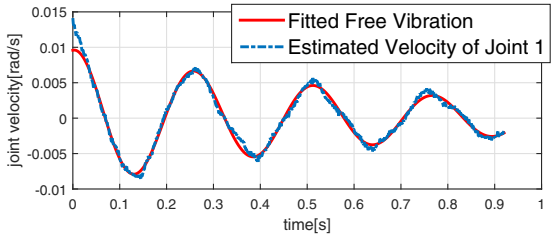

Fig. 7: Estimated Joint Velocity and Fitted Free Vibration.

The estimated frequency and damping ratio parameters of each joint are shown in Table.I. (where Jnt is short for Joint)

TABLE I: Estimated Frequency and Damping Ratio.

Parameter	Jnt 1	Jnt 2	Jnt 3	Jnt 4	Jnt 5	Jnt 6
Frequency [Hz]	3.7	4.7	5.9	4.3	4.4	4.4
Damping Ratio	0.11	0.12	0.07	0.14	0.23	0.14

The natural frequencies are around 4 Hz. The robot is performing rapid rest-to-rest motion within its workspace. The natural frequencies at different positions may be different. The same estimation is repeated at different positions, and the distribution of the mean natural frequencies of all the joints is shown in Fig.8. As shown in the figure, the frequencies are very close.

B. Robust Design

Due to the estimation error of the natural frequency and damping ratio error, the robust design of input shaping is necessary. Furthermore, as shown in IV-A the frequency and damping ratio parameters are different for different joints and different positions. In order to avoid poor performance due to a bad choice of parameters, robust design should be considered.

The specified insensitivity design of input shaping [17] is implemented in the experiment. 3 impulses are included in the input shaper. The natural frequency is chosen to be 4.5 Hz in the final design, and the damping ratio is chosen to be 0.05. The constraint of the SI shaper design is that the residual vibration level should not exceed 15% of the unshaped motion for the actual natural frequency $3.6\text{Hz} < \omega_0 < 5.4\text{Hz}$, which is a $\pm 20\%$ range. The parameters of the input shaper are: $A_1 = 0.3369$, $A_2 = 0.4069$, $A_3 = 0.2542$, $t_1 = 0$, $t_2 = 0.0891$, and $t_3 = 0.1766$. The SI shaper design is compared with the standard ZV shaper design in Fig.9. The x and y axis indicates the distribution of frequency and damping ratio parameters, and the z axis indicates the level of residual vibration. As shown in the figure, the vibration suppression performance is not sensitive to damping ratio. Comparing to ZV shaper, SI shaper is less sensitive to the change of frequency.

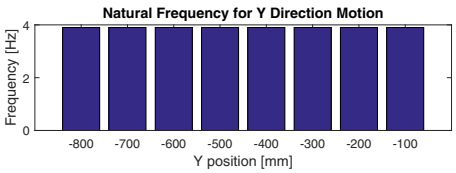

(a) Y direction

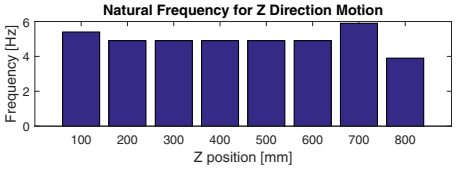

(b) Z direction

Fig. 8: Distribution of Natural Frequencies at Different Positions.

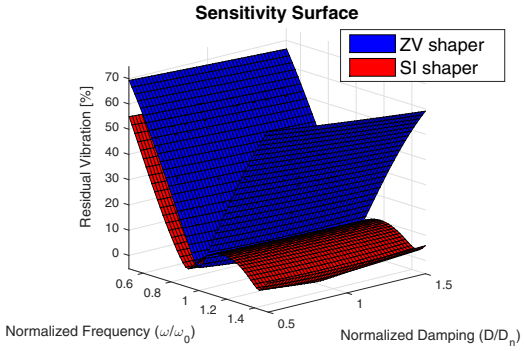

Fig. 9: Sensitivity Surface

C. Experiment Result

The proposed input shaping is implemented on the 6-axis industrial robot. The original motion command is accelerated by $t_{acc} = 0.2$. The input shaping is performed on normalized arc length as shown in Fig.2 in III-B. The Cartesian space motion command, unshaped motion command, and shaped motion command are compared in Fig.10. Comparing to unshaped motion, input shaping has effectively reduced the overshoot in z direction. This result can be observed more clearly in Fig.11. As shown in the figure, the overshoot has been reduced by 1.7 mm, which is about one third of the unshaped motion. From a practical point of view, the robot is considered to be settled when the residual vibration

is less than 1mm and the robot can start its work (e.g., spot welding). Since the amplitude of the residual vibration observed is very small, this level of vibration is tolerable for industrial robot applications. In this case the reduction of the overshoot becomes important as it can help avoid the collision due to path deviation.

The effect of input shaping in y direction is shown more clearly in Fig.12. While not included in the figure, the conventional SI shaper would have introduced a delayed response with a delay time of about 0.2 sec. The proposed method does not introduce such a delay.

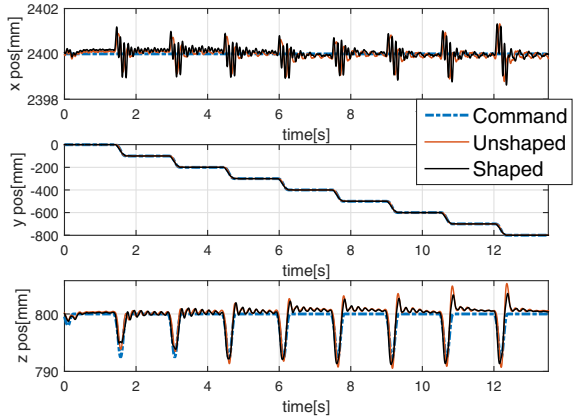

Fig. 10: Motion Command, Unshaped, and Shaped Motion.

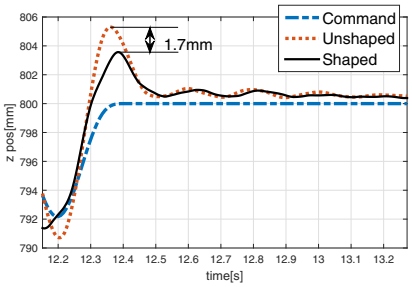

Fig. 11: Effect of the the Proposed Approach in Z Direction.

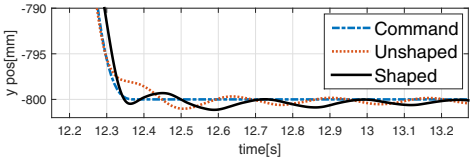

(a) Position

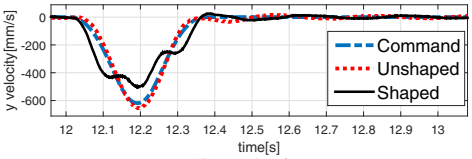

(b) Velocity

Fig. 12: Effect of the Proposed Approach in Y Direction.

V. Conclusion

In this paper, a zero time delay input shaping approach was proposed for smooth settling of an industrial robot. The proposed approach could fully compensate the time delay introduced by the conventional input shaping techniques. Another feature of the proposed approach was the ability to preserve the path of the unshaped motion command, which made it practical when applied to multi axis industrial robots. The proposed approach was implemented on a 6-axis industrial robot. The experiment results had shown that the proposed approach could effectively improve the performance of the robot by reducing the overshoot and no time delay was introduced.

References

[1] S. K. Dwivedy and P. Eberhard, "Dynamic analysis of flexible manipulators, a literature review," *Mechanism and machine theory*, vol. 41, no. 7, pp. 749–777, 2006.

[2] C. C. de Wit, B. Siciliano, and G. Bastin, *Theory of robot control*. Springer Science & Business Media, 2012.

[3] B. Siciliano and W. J. Book, "A singular perturbation approach to control of lightweight flexible manipulators," *The International Journal of Robotics Research*, vol. 7, no. 4, pp. 79–90, 1988.

[4] M. Benosman, G. Le Vey, L. Lanari, and A. De Luca, "Rest-to-rest motion for planar multi-link flexible manipulator through backward recursion," *Journal of dynamic systems, measurement, and control*, vol. 126, no. 1, pp. 115–123, 2004.

[5] N. C. Singer and W. P. Seering, "Preshaping command inputs to reduce system vibration," *Journal of Dynamic Systems, Measurement, and Control*, vol. 112, no. 1, pp. 76–82, 1990.

[6] A. Kamel, F. Lange, and G. Hirzinger, "New aspects of input shaping control to damp oscillations of a compliant force sensor," in *Robotics and Automation, 2008. ICRA 2008. IEEE International Conference on*. IEEE, 2008, pp. 2629–2635.

[7] W. Singhose, "Command shaping for flexible systems: A review of the first 50 years," *International Journal of Precision Engineering and Manufacturing*, vol. 10, no. 4, pp. 153–168, 2009.

[8] A. De Luca and P. Lucibello, "A general algorithm for dynamic feedback linearization of robots with elastic joints," in *Robotics and Automation, 1998. Proceedings. 1998 IEEE International Conference on*, vol. 1. IEEE, 1998, pp. 504–510.

[9] F. Ghorbel, J. Y. Hung, and M. W. Spong, "Adaptive control of flexible-joint manipulators," *Control Systems Magazine, IEEE*, vol. 9, no. 7, pp. 9–13, 1989.

[10] A. De Luca and G. Ulivi, "Iterative learning control of robots with elastic joints," in *Robotics and Automation, 1992. Proceedings., 1992 IEEE International Conference on*. IEEE, 1992, pp. 1920–1926.

[11] W. Chen and M. Tomizuka, "Dual-stage iterative learning control for mimo mismatched system with application to robots with joint elasticity," *Control Systems Technology, IEEE Transactions on*, vol. 22, no. 4, pp. 1350–1361, 2014.

[12] W. J. Book, "Controlled motion in an elastic world," *Journal of dynamic systems, measurement, and control*, vol. 115, no. 2B, pp. 252–261, 1993.

[13] W. E. Singhose, W. P. Seering, and N. C. Singer, "Input shaping for vibration reduction with specified insensitivity to modeling errors," *Japan-USA Sym. on Flexible Automation*, vol. 1, pp. 307–13, 1996.

[14] Y. Hu, B. Wu, J. Vaughan, and W. Singhose, "Oscillation suppressing for an energy efficient bridge crane using input shaping," in *Control Conference (ASCC), 2013 9th Asian*. IEEE, 2013, pp. 1–5.

[15] F. Boeren, D. Bruijnen, N. van Dijk, and T. Oomen, "Joint input shaping and feedforward for point-to-point motion: Automated tuning for an industrial nanopositioning system," *Mechatronics*, vol. 24, no. 6, pp. 572–581, 2014.

[16] J. Vaughan, J. Yoo, N. Knight, and W. Singhose, "Multi-input shaping control for multi-hoist cranes," in *American Control Conference (ACC), 2013*. IEEE, 2013, pp. 3449–3454.

[17] J. Vaughan, A. Yano, and W. Singhose, "Comparison of robust input shapers," *Journal of Sound and Vibration*, vol. 315, no. 4, pp. 797–815, 2008.